Analyst

PAPER

View Article Online
View Journal | View Issue

Cite this: *Analyst*, 2026, **151**, 2324

Magnetic-aminopropyltriethoxysilane-sulfanilamide: a new functional sorbent for selective preconcentration of sulfonylurea antidiabetic drugs in biological samples

Songül Ulusoy,*[a] Şule İrem Altunbaş,[b] Aslıhan Gürbüzer,[c] Ümmügülsüm Polat[b] and Halil İbrahim Ulusoy [b]

A highly selective and sensitive analytical strategy was established for the trace quantification of two oral antidiabetic drugs, gliclazide (GLZ) and glimepiride (GLM). The procedure integrates magnetic solid-phase extraction (MSPE) with high-performance liquid chromatography coupled to diode array detection (HPLC-DAD). In this approach, a newly engineered magnetic-aminopropyltriethoxysilane-sulfanilamide (Fe_3O_4@APTES-sulfanilamide) was synthesized and utilized as an innovative adsorbent. Sulfanilamide as a functional molecule on the surface has been used for the first time in this study. The hybrid structure, consisting of a Fe_3O_4 magnetic core and a sulfanilamide-functionalized silane shell, provides strong binding affinity toward sulfonylurea compounds through synergistic hydrogen bonding and π–π interactions. Optimization studies were carried out to achieve the best extraction efficiency by adjusting experimental variables such as solution pH, adsorption and desorption times, and solvent composition. Under the final working conditions (pH 6.0; desorption with an acetonitrile–methanol mixture), both target analytes were effectively preconcentrated prior to chromatographic determination. Separation was accomplished using an isocratic elution system containing 10% methanol, 40% phosphate buffer (pH 3.0), and 50% acetonitrile, with UV detection at 219 and 256 nm. The developed protocol demonstrated excellent linearity, remarkable enrichment factors, and very low detection limits. Precision studies yielded RSD values below 3.5% (n = 3, 100 ng mL^{-1}). The reliability of the proposed method was further validated by its successful application to both synthetic and human urine samples, giving satisfactory recovery results. This newly designed Fe_3O_4@APTES-sulfanilamide -based MSPE coupled with HPLC-DAD provides a robust, time-efficient, and eco-friendly platform for the determination of trace oral antidiabetic drugs in complex biological matrices.

Received 30th December 2025,
Accepted 25th February 2026

DOI: 10.1039/d5an01377a

rsc.li/analyst

1. Introduction

Diabetes mellitus is a multifactorial metabolic disorder arising from the interplay of genetic predisposition and environmental factors, and it is clinically characterized by persistent hyperglycemia resulting from impaired insulin secretion, defective insulin action, or both mechanisms.[1] The disease manifests with classical symptoms such as polyuria, polydipsia, fatigue, and metabolic imbalance, and it remains one of the most critical global public health challenges according to the World Health Organization.[2,3] Chronic hyperglycemia is associated with long-term microvascular and macrovascular complications, necessitating continuous therapeutic monitoring and effective glycemic control strategies.[4,5]

Sulfonylureas constitute one of the most widely prescribed classes of oral antidiabetic drugs for the management of Type II diabetes mellitus. These agents act primarily as insulin secretagogues by stimulating pancreatic β-cells, thereby enhancing endogenous insulin release. Among them, gliclazide and glimepiride are prominent second-generation sulfonylureas, offering improved potency, selectivity, and pharmacokinetic profiles compared with earlier derivatives.[6–8] In addition to their pancreatic effects, these drugs have been reported to exert extra-pancreatic actions, including enhancement of peripheral insulin sensitivity and facilitation of glucose uptake in target tissues.[9,10] Owing to their widespread clinical use and pharmacological significance, reliable analytical methods are

[a]*Department of Pharmacy, Vocational School of Health Service, Sivas Cumhuriyet University, Sivas, Türkiye. E-mail: songululusoy@cumhuriyet.edu.tr*
[b]*Department of Analytical Chemistry, Faculty of Pharmacy, Sivas Cumhuriyet University, Sivas, Türkiye*
[c]*Department of Plant and Animal Production, Vocational School of Technical Services, Sivas Cumhuriyet University, Sivas, Türkiye*

required for their determination in pharmaceutical formulations and biological matrices.

Several analytical approaches have been reported for the determination of sulfonylurea drugs, including spectrophotometry,[11] capillary electrophoresis,[12] and chromatographic techniques such as HPLC-UV,[13] HPLC-PDA,[14] and LC-MS/MS.[15] While these methods provide acceptable sensitivity and selectivity, many of them require extensive sample preparation, large solvent consumption, or sophisticated instrumentation. In particular, the direct analysis of biological matrices remains challenging due to matrix interferences, low analyte concentrations, and inadequate preconcentration capability. These limitations highlight the need for selective, efficient, and environmentally sustainable sample preparation strategies prior to chromatographic determination.

Solid-phase extraction (SPE) is a widely applied sample preparation technique that offers numerous advantages, including methodological flexibility and compatibility with a wide range of adsorbent materials. Compared to liquid–liquid extraction, the SPE approach requires smaller volumes of organic solvents and shorter processing times, thereby making it more environmentally sustainable and operationally efficient.[16,17] Furthermore, the use of minimal quantities of sorbent materials allows for higher recovery rates and enrichment factors. The two commonly employed SPE configurations are batch and column techniques.[18–21] In recent years, magnetic nanoparticles (MNPs) have gained significant attention as sorbent materials in SPE applications due to their distinctive physicochemical characteristics.[22] Owing to their exceptionally large surface area, magnetic nanoparticles typically exhibit high adsorption capacities toward target analytes. Moreover, their surfaces can be readily functionalized with specific ligands, enabling selective interaction and binding with target molecules within complex sample matrices.[23,24]

A notable advantage of MNP-based extraction lies in their facile separation from aqueous media under the influence of an external magnetic field, eliminating the need for conventional filtration or centrifugation steps. Unlike traditional solid-phase microextraction, magnetic solid-phase extraction (MSPE) does not require the use of packed columns, thereby circumventing the operational difficulties associated with sorbent loading, replacement, and desorption.[25,26] The surfaces of magnetic sorbents can be modified depending on the molecular structure of target molecules. In this way, the surface of the nanoparticles becomes more compatible with the target molecules. Depending on the chemical structure of the molecule used in the surface coating, nanoparticles can be endowed with hydrophilic, hydrophobic, negatively charged, or positively charged characteristics. Scientists around the world conducting research in this field are carrying out numerous studies aimed at developing novel and functional materials.[27–29] Our research group also has published several articles on this subject.[30–33] In the present study, the surface modification of magnetic nanoparticles was performed using a sulfanilamide molecule. Although sulfanilamide is conventionally known as an antibiotic compound, its ideal molecular structure provided a favorable interaction platform for the target drug molecules. The ability of structurally similar molecules to bind to silanized groups is well documented and supported by the literature.[34,35] Following extraction, magnetic nanoparticles can be completely isolated from the solution using a simple external magnet, which significantly simplifies the analytical workflow. Furthermore, due to their reusable and recyclable nature, magnetic nanoparticles represent a cost-effective and environmentally sustainable alternative for modern analytical separation processes.

Surface functionalization using APTES represents one of the most employed silanization strategies for magnetic nanoparticles due to its chemical stability and ease of modification. However, APTES alone primarily serves as a linker layer rather than a selective recognition interface. In the present study, this conventional platform was further engineered through the immobilization of sulfanilamide moieties. The rationale behind this design lies in the structural similarity and complementary interaction potential between sulfanilamide functional groups and sulfonylurea antidiabetic drugs, enabling enhanced hydrogen bonding, dipole–dipole, and π–π interactions. To the best of our knowledge, the use of sulfanilamide-functionalized Fe_3O_4@APTES magnetic nanoparticles as a selective MSPE sorbent for gliclazide and glimepiride has not been previously documented, thereby providing a new molecularly oriented extraction approach.

The distinctive aspect of this study lies in the design and synthesis of a novel Fe_3O_4@APTES-sulfanilamide magnetic nanocomposite, which has not been previously reported as a sorbent for sulfonylurea-type oral antidiabetic drugs. The material provides enhanced selectivity and extraction efficiency due to the synergistic interactions between sulfanilamide functional groups and the target analytes. Integrating this innovative sorbent into an MSPE–HPLC-DAD platform offers a rapid, sensitive, and eco-friendly analytical approach suitable for trace-level monitoring of antidiabetic agents in complex biological matrices.

2. Materials and methods

2.1. Chemicals and materials

All reagents and chemicals used throughout this research were of analytical grade with a minimum purity of 99.5%. Iron(II) chloride and iron(III) chloride, (3-aminopropyl)triethoxysilane (APTES), and sulfanilamide were obtained from Sigma-Aldrich (St. Louis, MO, USA). Deionized water with a resistivity of 18.2 MΩ cm, produced by a MES Minipure Dest-Up purification unit, was utilized in all synthesis and analytical stages.

Chromatography-grade solvents, including methanol and acetonitrile, were also supplied by Sigma-Aldrich (St. Louis, MO, USA). Britton–Robinson (BR) buffer solutions covering the pH range of 2.0–10.0 were freshly prepared from a 0.02 M mixed acid solution consisting of boric, phosphoric, and acetic acids. The required pH values were adjusted by the gradual addition of 0.1 M sodium hydroxide while continuously moni-

toring with a calibrated pH meter. Stock standard solutions of gliclazide (GLZ) and glimepiride (GLM) were prepared at concentrations of 1000 μg mL^{-1} in analytical-grade methanol (Sigma-Aldrich). These solutions were kept in amber glass vials at +4 °C to prevent degradation due to light exposure.

2.2. Instrumentation

Morphological and elemental characterization of the synthesized materials was carried out using a Philips XL30 scanning electron microscope (SEM) coupled with an EDAX energy-dispersive X-ray (EDX) detector, providing high-resolution imaging and precise compositional analysis. To ensure thorough homogenization of solutions, a Fisher Scientific digital orbital shaker (Fisherbrand) and a Velp Scientifica ZX3 vortex mixer (Model F20220176) were employed. All pH measurements were conducted using a glass-calomel electrode pH meter (Mettler Toledo, Columbus, OH, USA), calibrated before each measurement. Sample dispersion and preparation were facilitated by an ultrasonic water bath (Kudos, China) to guarantee uniform mixing.

Chromatographic analyses were performed on a Shimadzu LC-20AD high-performance liquid chromatography (HPLC) system (Shimadzu, Tokyo, Japan) equipped with a photodiode array (PDA) detector (SPD-M20A), an autosampler (SIL-20AC), a column oven (CTO-10AS), and a high-pressure pump (LC-20AD). Data acquisition, processing, and integration were managed using the LC Solution software (Shimadzu), allowing for precise control of experimental conditions and real-time monitoring of chromatographic performance.

2.3. HPLC analysis conditions for gliclazide and glimepiride

Literature data on gliclazide and glimepiride were consulted, and experimental parameters were systematically optimized to achieve the direct quantification of these antidiabetic agents using an HPLC system. A Phenomenex C18 column was selected as the most suitable stationary phase for this purpose. To identify the optimal mobile phase composition, aqueous solutions of various organic solvents containing buffers at different pH values were tested. Both isocratic and gradient elution strategies were evaluated through multiple trials to achieve well-resolved peaks and accurate quantification. The optimized HPLC operating conditions are summarized in Table 1. These results confirm the suitability of the optimized method for precise and reproducible analysis of the target analytes.

Table 1 HPLC operating conditions for target molecules

Parameter	Value
HPLC mode	Isocratic
Eluent	10% methyl alcohol 40% (0.02 M KH_2PO_4, pH 3.0) 50% acetonitrile
Eluent flow rate	1.0 mL min^{-1}
Run time	14 min
Column	Phenomex C-18 (150 × 5 mm, 5 μm)
Column temperature	45 °C
Injection volume	10 μL

2.4. Synthesis of the solid phase support material Fe_3O_4@APTES-sulfanilamide

The synthesis protocol employed in this study follows procedures reported in our previous works.[36–38] Initially, 8.10 g of $FeCl_3{\cdot}6H_2O$ and 2.98 g of $FeCl_2{\cdot}4H_2O$ were dissolved in a mixture of 50 mL of 0.1 M HCl and 100 mL of ethanol. The solution was stirred at 750 rpm and maintained at 65 °C under a nitrogen atmosphere to provide an inert environment. Subsequently, 25 mL of ammonia solution was slowly added dropwise to the vigorously stirred mixture, resulting in the formation of magnetic nanoparticles. The black Fe_3O_4 precipitate was then separated using an external magnetic field, thoroughly rinsed with a water/ethanol mixture, and dried in an oven at 60 °C for 6 hours.

For surface functionalization, 2 g of the dried Fe_3O_4 nanoparticles were dispersed in 50 mL of water : ethanol(1 : 1), followed by the addition of 3 mL of concentrated ammonia and 2 mL of (3-aminopropyl)triethoxysilane (APTES). Building on previous experimental findings and literature reports, further modification was performed to enhance the nanoparticles' affinity toward the target analytes. Specifically, 250 mg of sulfanilamide dissolved in 50 mL of ethanol was added, and the mixture was stirred at room temperature for 6 hours. The resulting functionalized nanoparticles were then repeatedly washed with an ethanol/water mixture and dried under ambient conditions.

2.5. The developed MSPE–HPLC based method

Optimal extraction performance was achieved through systematic optimization of key parameters, including sample pH, adsorption and desorption conditions. For the extraction procedure, 50 mg of the magnetic solid-phase sorbent (Fe_3O_4@APTESsulfanilamide) was accurately weighed and placed into 50 mL falcon tubes. 20 mL of sample solution including target molecules (in the range of 10.0–900.0 ng mL^{-1}) and 2 mL of pH 6.0 buffer were added to each tube. The total volume in each tube was adjusted to 50 mL with deionized water. The tubes were securely capped and rotated at 50 rpm for 50 minutes to allow thorough mixing and adsorption of the analytes onto the magnetic sorbent.

After the adsorption period, the tubes were positioned within an external magnetic holder to separate the aqueous phase, which was carefully removed using a pipette. Desorption of the retained analytes was performed by adding 500 μL of a mixture of acetonitrile : methanol (1 : 1) to each tube, followed by 60 seconds of vortexing. The resulting solution containing the eluted analytes was collected under the magnetic field using a syringe, filtered through a 0.45 μm PTFE syringe filter, and transferred into HPLC vials. The enriched samples of GLZ and GLM were subsequently subjected to HPLC analysis under the previously optimized chromatographic conditions.

2.6. Preparation for synthetic and real urine

Synthetic urine solutions were prepared based on previously reported formulations to[39–41] mimic the composition of human urine, serving as a relevant matrix for the evaluation of antidiabetic drug residues. These solutions were subsequently employed during the experimental application phase.

2.6.1. Preparation of synthetic urine. To obtain 1 L of synthetic urine, 25 g of urea, 1.08 g of $CaCl_2{\cdot}2H_2O$, 1 g of NH_4Cl, 1.6 g of KCl, 1.4 g of Na_2SO_4, 1.4 g of KH_2PO_4, and 2.92 g of NaCl were accurately weighed and dissolved in a portion of distilled water. The mixture was then transferred to a 1 L volumetric flask and diluted to the final volume. The pH was adjusted to 6.0 using 0.1 M NaOH, and the solution was stored in amber glass bottles at +4 °C until further use.

2.6.2. Collection of human urine. The urine samples from a healthy volunteer, who abstained from any medication and provided informed consent regarding the experimental procedure and the nature of the study, were collected into capped test tubes and immediately analyzed. For this study, a sample of "normal" urine was obtained from a 23-year-old volunteer on June 2, 2022, and stored under appropriate conditions prior to experimental application.

3. Results and discussion

A highly sensitive analytical procedure was established for the quantification of trace levels of GLZ and GLM in oral OAD formulations, utilizing magnetic solid-phase extraction (MSPE) for sample enrichment in combination with HPLC-DAD detection. The main aim of this methodology was to selectively isolate the target compounds from complex matrices by maximizing their adsorption onto the magnetic sorbent, followed by efficient elution to ensure complete recovery. Comprehensive preliminary studies were carried out to optimize key experimental parameters essential for achieving these objectives. Attention was given to developing a rapid, simple, and environmentally friendly separation procedure, minimizing the use of organic solvents while enhancing analyte preconcentration. These efforts enabled the enrichment of analytes to concentrate within the detection limits of the HPLC system. Consequently, a robust chromatographic method was established through systematic optimization of all relevant operational variables.

The interaction mechanism between GLZ/GLM and the Fe_3O_4@APTES-sulfanilamide sorbent can be attributed to the presence of multiple surface functional groups introduced by APTES and sulfanilamide. The amine groups from APTES and the sulfonamide moieties on the surface can establish hydrogen bonding and electrostatic interactions with functional groups (*e.g.*, carbonyl and sulfonyl) present in the analytes. The aromatic ring of sulfanilamide may also contribute *via* π–π stacking with the aromatic regions of GLZ and GLM, enhancing interaction strength. Previous studies on amine-functionalized silica/magnetic adsorbents have reported that amino groups significantly influence adsorption behavior through electrostatic attraction and hydrogen bonds between surface $-NH_2$ and analyte molecules (*e.g.*, adsorption of organic contaminants onto APTES-modified magnetic silica nanoparticles)[42] and similar sulfanilamide-functionalized magnetic nanoparticles have been effectively prepared and characterized to interact with target species through surface functional groups, demonstrating the role of covalently attached organic moieties in binding performance.[43] These combined interactions explain the high extraction efficiency and selectivity observed in the present study.

3.1. Characterization of Fe_3O_4 and Fe_3O_4@APTES-sulfanilamide nanoparticles

The FTIR spectra of pristine Fe_3O_4 and surface-functionalized Fe_3O_4@APTESsulfanilamide nanocomposites are presented in Fig. 1. The characteristic absorption band observed at approximately 580 cm^{-1} corresponds to the Fe–O stretching vibration of the magnetite core, confirming the retention of the crystalline Fe_3O_4 structure after surface modification.[44] In the Fe_3O_4@APTES-sulfanilamide spectrum, several new absorption bands appear, indicating successful functionalization. The broad band around 3400–3200 cm^{-1} is attributed to the overlapping N–H and O–H stretching vibrations, which may arise from the surface amino groups of APTES and adsorbed water molecules.[45] The absorption peaks observed near 2920 cm^{-1} correspond to the C–H stretching of aliphatic $-CH_2$ groups from the propyl chain of APTES, confirming the attachment of organic moieties on the magnetic surface.[46] The band appearing at 1635 cm^{-1} can be ascribed to N–H bending or C═N stretching vibrations, indicating the interaction between the amine and sulfanilamide functionalities. The strong bands detected in the range of 1100–1000 cm^{-1} are characteristic of Si–O–Si and Si–O–Fe linkages, confirming that APTES molecules were covalently bonded to the Fe_3O_4 surface through silanol condensation.[47] Moreover, the absorption at 1150–1200 cm^{-1} is assigned to the S═O stretching vibration of sulfanilamide groups, validating the successful immobiliz-

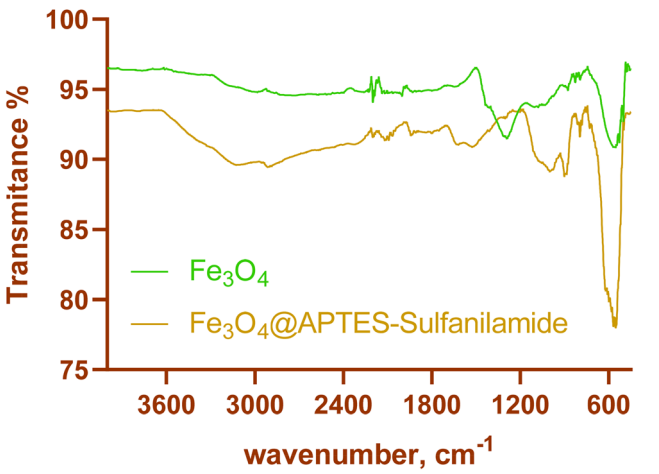

Fig. 1 FTIR spectrum of the developed magnetic material.

ation of sulfanilamide moieties on the APTES-modified magnetic nanoparticles.[48] These findings collectively confirm that the surface modification process was effectively accomplished without altering the magnetic core structure of Fe_3O_4.

The XRD patterns of pure Fe_3O_4 and surface-functionalized Fe_3O_4@APTESsulfanilamide nanoparticles are shown in Fig. 2. Both samples exhibit characteristic diffraction peaks at approximately 2θ = 30.2°, 35.5°, 43.2°, 53.5°, 57.1°, and 62.7°, corresponding to the (220), (311), (400), (422), (511), and (440) crystallographic planes of the cubic spinel structure of magnetite (JCPDS card No. 19-0629). These reflections confirm that the magnetic core retains its crystalline nature following surface modification.[49] A slight decrease in peak intensity and a marginal broadening of the diffraction lines are observed for Fe_3O_4@APTESsulfanilamide compared to those of bare Fe_3O_4, which can be attributed to the formation of an amorphous organosilane layer surrounding the magnetic nanoparticles and to a partial reduction in coherent crystallite size. The absence of additional diffraction peaks indicates that neither APTES functionalization nor sulfanilamide grafting was induced any phase transformation or impurity formation in the magnetite structure.

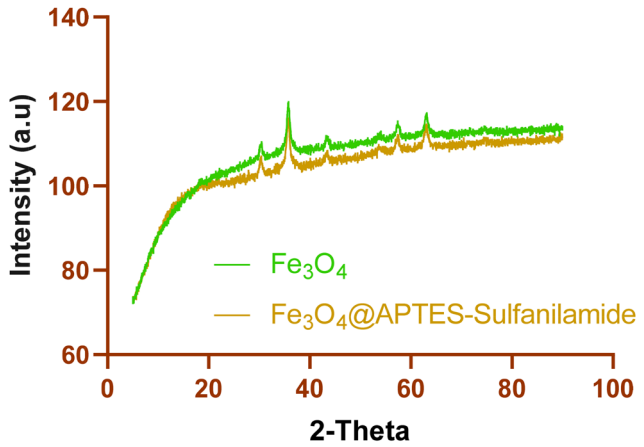

Fig. 2 XRD analysis of the developed magnetic material.

The surface morphology of the pristine and functionalized magnetite nanoparticles was examined by scanning electron microscopy (SEM), as shown in Fig. 3. The pristine Fe_3O_4 nanoparticles (Fig. 3A) exhibit a nearly spherical morphology with a uniform distribution and a tendency to form compact agglomerates due to the high surface energy and magnetic dipole–dipole interactions between individual particles. In contrast, the Fe_3O_4@APTESsulfanilamide nanocomposite (Fig. 3B) displays a slightly rougher and more irregular surface texture, which can be attributed to the successful coating of APTES and subsequent immobilization of sulfanilamide groups on the nanoparticle surface. The presence of a thin organic layer and the increased particle clustering are consistent with the formation of a surface-modified shell around the magnetic core, without significant alteration of the overall morphology. These morphological observations support the FTIR and XRD results, confirming the effective surface

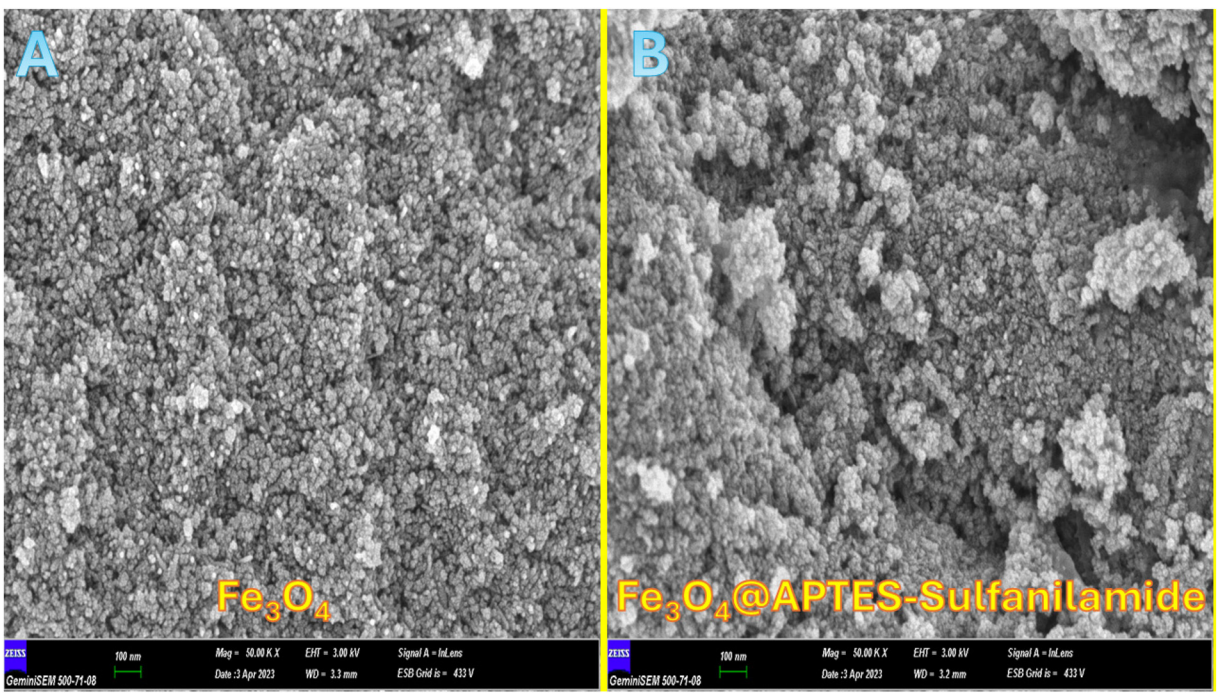

Fig. 3 SEM images of the developed magnetic sorbent. SEM micrographs of (A) bare Fe_3O_4 magnetic nanoparticles, (B) APTES-modified Fe_3O_4, and sulfanilamide-functionalized magnetic nanoparticles. The images were recorded at enhanced magnification to better visualize the particle morphology and surface modification effects. Scale bars represent 100 nm.

functionalization of Fe_3O_4 nanoparticles while preserving their nanostructured integrity.

3.2. Optimization of the developed method

3.2.1. Effect of sample pH. The pH of the extraction medium plays a crucial role in governing the interaction between the analyte molecules and the surface of the magnetic sorbent, as it influences both the ionization state of the drugs and the surface charge of the nanoparticles. To systematically investigate this effect, experiments were conducted across a pH range of 2.0–10.0 using Britton–Robinson (BR) buffer solutions. For each trial, 2 mL of the corresponding buffer and 20 mL of model solution including GLZ and GLM molecules at 250 ng mL^{-1} were added into 50 mL Falcon tubes containing 50 mg of the magnetic phase.

As illustrated in Fig. 4, the extraction efficiency exhibited a pronounced dependence on the solution pH. The optimal enrichment was achieved at pH 6.0, where the balance between the surface charge of the magnetic nanoparticles and the ionization state of the analytes favored maximum adsorption. Considering the pK_a values of gliclazide (≈5.8)[50] and glimepiride (≈6.2),[51] both compounds exist predominantly in their neutral or partially deprotonated forms at pH 6.0, which promotes hydrophobic and hydrogen-bonding interactions with the functional groups present on the nanoparticle surface. At lower pH values (<4), protonation of the surface $-NH_2$ and –OH groups leads to increased electrostatic repulsion and reduced analyte affinity, while at higher pH (>8), excessive deprotonation diminishes the availability of active binding sites and weakens interaction strength.[52,53]

Therefore, pH 6.0 was selected as the optimal condition for subsequent enrichment experiments, ensuring a favorable electrostatic environment and efficient mass transfer between the magnetic sorbent and the oral antidiabetic drug molecules.

3.2.2 Optimization of adsorption time. The adsorption or shaking time directly governs the rate and extent of interaction between the analyte molecules and the surface-active sites of the magnetic sorbent. During this stage, the transfer of the analyte species from the bulk solution to the sorbent surface proceeds through diffusion and surface binding, ultimately reaching an equilibrium between adsorption and desorption processes. Therefore, adequate contact time is essential to achieve maximum enrichment efficiency and ensure that all active sites on the magnetic material are effectively utilized. To evaluate the influence of adsorption time, ten parallel experiments were conducted under identical experimental conditions, varying only the shaking duration between 1 and 120 minutes. The concentrations of the oral antidiabetic drugs (GLZ and GLM), pH, sorbent dosage, and solvent composition were maintained constant. As shown in Fig. 5, extraction efficiency initially increased sharply with contact time due to enhanced molecular diffusion and progressive occupation of the active surface sites. Beyond approximately 40 minutes, the signal intensity reached a plateau, indicating that equilibrium had been established between the adsorption and desorption processes. Prolonged shaking beyond this point did not result in a significant increase in recovery, confirming that 40 minutes was sufficient to achieve equilibrium adsorption.

This behavior suggests that the interaction between the analytes and the Fe_3O_4@APTES-sulfanilamide surface is primarily governed by a combination of electrostatic and hydrogen-bonding interactions, reaching equilibrium within a moderate time frame. Accordingly, 50 minutes was selected as the optimal adsorption time for subsequent enrichment experiments.

3.2.3 Optimization of desorption conditions. The choice and volume of the desorption solvent represent critical parameters in magnetic solid-phase extraction (MSPE), as they directly determine the efficiency with which analytes retained

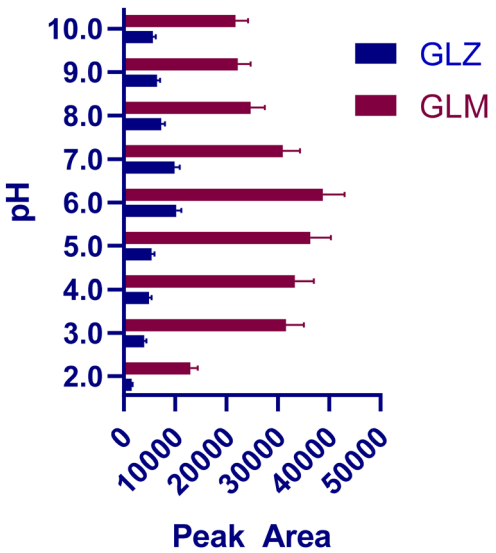

Fig. 4 The optimization of pH for the MSPE based method.

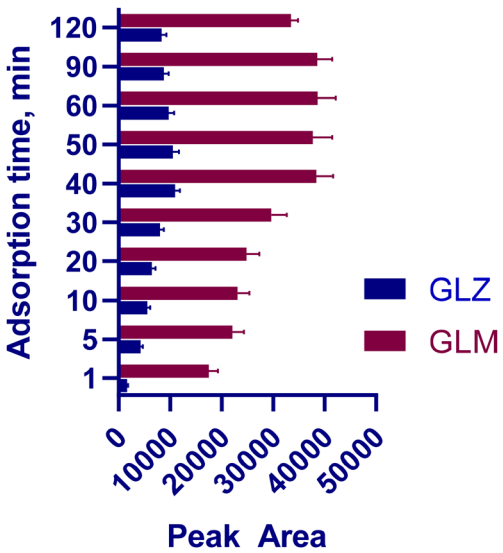

Fig. 5 Suitable adsorption time for the proposed method.

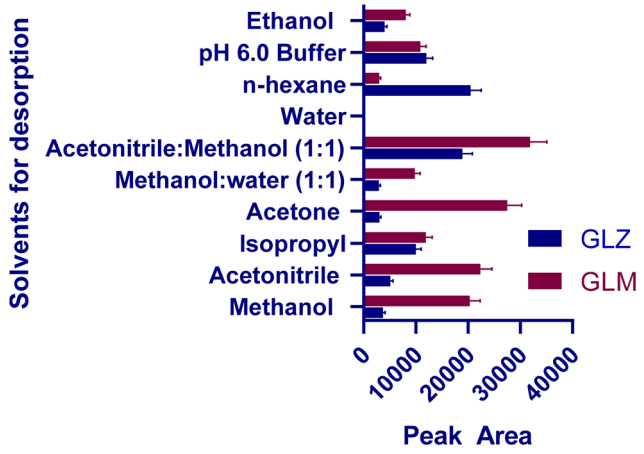

Fig. 6 Appropriate solvent selection for the proposed method.

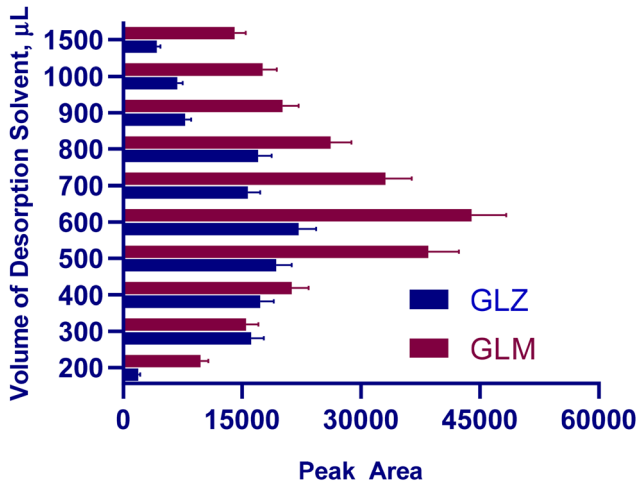

Fig. 7 Optimization of the volume of the desorption solvent.

on the sorbent surface are released back into the liquid phase for chromatographic detection. Effective desorption requires that the solvent not only disrupts the intermolecular interactions between the analyte and sorbent surface but also provides sufficient solubility for the analyte molecules to prevent re-adsorption or precipitation prior to HPLC injection.

To assess the effect of the solvent type on desorption efficiency, a series of experiments was conducted using ten parallel samples under identical conditions, varying only the solvent composition. The solvents evaluated included distilled water, methanol, acetonitrile, ethanol, isopropanol, *n*-hexane, acetone, pH 6.0 Britton–Robinson buffer, and a 1 : 1 (v/v) acetonitrile–methanol mixture. Following the adsorption of GLZ and GLM onto the Fe_3O_4@APTES-sulfanilamide sorbent, each solvent was tested as an eluting phase under otherwise identical conditions. As illustrated in Fig. 6, the highest and most distinct chromatographic peaks were obtained when a 1 : 1 (v/v) mixture of acetonitrile and methanol was used as the desorption solvent. This binary solvent system effectively balanced polarity and elution strength, facilitating disruption of hydrogen-bonding and van der Waals interactions between the analytes and the functionalized sorbent surface. Purely aqueous or less polar solvents, such as *n*-hexane and isopropanol, yielded significantly lower recoveries due to insufficient solvation of the relatively polar sulfonylurea structures of the analytes. Consequently, the 1 : 1 acetonitrile–methanol mixture was selected as the optimal desorption medium for all subsequent enrichment and analytical experiments, providing both high recovery and sharp chromatographic peak resolution.

In addition to the solvent type, the desorption solvent volume plays a decisive role in determining the overall recovery of analytes from the magnetic sorbent surface. An insufficient solvent volume may not fully wet and penetrate the sorbent matrix, resulting in incomplete elution of adsorbed analytes. Conversely, an excessively large volume can lead to sample

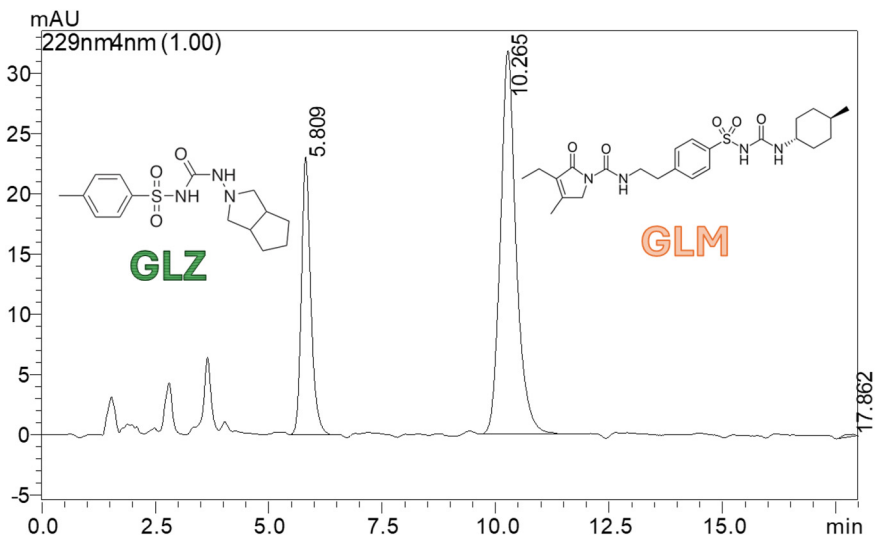

Fig. 8 Chromatograms of gliclazide and glimepiride molecules (250 ng mL^{-1}) obtained under ideal conditions after MSPE.

dilution, reducing preconcentration efficiency and thereby lowering chromatographic peak intensity. To establish the optimal desorption volume, a series of experiments was performed using the previously optimized 1 : 1 (v/v) acetonitrile–methanol mixture as the eluent. The desorption volume was varied between 200 and 1500 μL, while maintaining all other parameters constant, including adsorption time, sorbent mass, and desorption time.

As shown in Fig. 7, analyte peak areas initially increased with increasing solvent volume, reflecting improved wetting and diffusion into the sorbent structure. Maximum signal intensity and recovery for both GLZ and GLM were achieved at a desorption volume of 600 μL, indicating efficient disruption of analyte–sorbent interactions and complete transfer of analytes into the liquid phase. Beyond this volume, peak areas exhibited a pronounced decline due to the dilution effect. Therefore, 600 μL of the 1 : 1 acetonitrile–methanol mixture was selected as the optimal desorption solvent volume for subsequent experiments, providing the best balance between elution efficiency and enrichment factor.

3.2.4 Optimization of desorption time. The duration of the desorption process, referred to as elution time, is a key factor in ensuring complete transfer of analytes from the magnetic sorbent into the solvent. Inadequate elution time may result in incomplete recovery due to insufficient disruption of analyte–sorbent interactions, while excessively long elution may lead to unnecessary solvent handling without significant gain in recovery. To investigate the optimal elution time, the tubes were subjected to vortexing for varying durations ranging from 10 to 120 seconds, keeping all other parameters constant. Maximum peak areas were achieved at 60 seconds, beyond which no significant improvement in peak intensity was observed, indicating that equilibrium desorption had been reached. These findings confirm that 60 seconds of elution is sufficient to efficiently transfer the analytes into the solvent

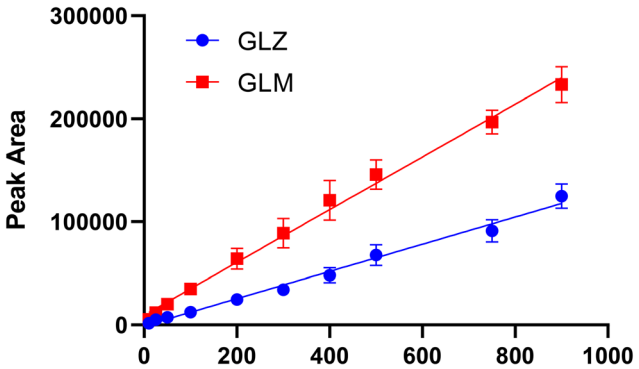

Fig. 9 Linear working range of the developed method.

Table 2 Analytical parameters of the proposed method

	Without MSPE method		With MSPE method	
Parameter	GLZ	GLM	GLZ	GLM
Linear range	1.0–20.0 μg mL^{-1}	1.0–20.0 μg mL^{-1}	10.0–900.0 ng mL^{-1}	10.0–900.0 ng mL^{-1}
LOD[a]	0.32 μg mL^{-1}	0.38 μg mL^{-1}	3.58 ng mL^{-1}	3.63 ng mL^{-1}
LOQ[a]	0.85 μg mL^{-1}	0.92 μg mL^{-1}	9.85 ng mL^{-1}	9.78 ng mL^{-1}
RSD (%)	5.30	7.09	5.2	6.5
Calibration sensitivity	24.3	36.8	2063.1	3510.7
Correlation coefficient (R^2)	0.9985	0.9890	0.9901	0.9948
Pre-concentration factor[b]	—	—	83.3	83.3
Enhancement factor[c]	—	—	84.9	95.4

[a] It was calculated as stated in the ICH guidelines source. [b] Pre-concentration factor; it was calculated by taking the ratio of the initial aqueous phase volume (50 mL) to the volume obtained after enrichment (0.6 mL). [c] The enhancement factor was determined by dividing the slope of the calibration curve obtained using the MSPE method by that of the calibration curve obtained without MSPE.

Table 3 Application of the developed method to urine samples

		Found[a] (ng mL^{-1})		RSD %		Recovery %	
Examples	Added ng mL^{-1}	GLZ	GLM	GLZ	GLM	GLZ	GLM
Synthetic urine	0.0	<LOD	<LOD	—	—	—	—
	200.0	192.4 ± 12.5	196.5 ± 10.9	6.5	5.5	96.2	98.3
	400.0	412.5 ± 28.4	409.5 ± 21.1	6.9	5.2	103.1	102.4
Real urine	0.0	<LOD	<LOD	—	—	—	—
	200.0	202.5 ± 12.4	212.6 ± 12.4	6.1	5.2	101.3	106.3
	400.0	374.8 ± 19.4	391.5 ± 13.2	5.8	3.4	93.7	97.9

[a] Mean of 3 repeated measurements ± standard deviation

while maintaining sample concentration and minimizing unnecessary dilution.

3.3. Analytical performance criteria of the developed method

Following the optimization of the solid-phase extraction conditions, the linear dynamic range of the developed method was evaluated using standard solutions of GLZ and GLM at varying concentrations. MSPE experiments were performed for each concentration, and the analyte responses were recorded using HPLC-DAD detection. Gliclazide was monitored at 219 nm, while glimepiride was measured at 256 nm. Representative chromatograms of model solutions after MSPE demonstrate the well-defined peaks of GLZ and GLM as shown in Fig. 8.

Once the MSPE parameters were optimized, the analytical validation of the developed method was systematically performed in accordance with the International Council for Harmonization (ICH) guidelines for analytical procedure validation.[54] The validation process included the evaluation of linearity, accuracy (recovery), precision (expressed as %RSD), limit of detection (LOD), and limit of quantification (LOQ). The analytical performance data obtained for GLZ and GLM under the optimized conditions are summarized in Table 2. For comparison purposes, a direct analytical procedure without the MSPE step was performed. Standard and sample solutions were prepared at the same concentration levels and directly injected into the HPLC system under the optimized chromatographic conditions described above. No preconcentration or extraction step was applied. The obtained peak areas were used to evaluate the enhancement effect of the MSPE procedure by comparing signal intensities and sensitivity parameters.

As described earlier, the chromatographic method was initially optimized using model solutions prior to its coupling with the MSPE procedure, allowing for a comparative assessment of analytical performance before and after enrichment. The application of MSPE significantly improved the method's sensitivity, extending its quantification capability from the microgram to the nanogram per milliliter range. Calibration curves were established by applying the developed method to standard solutions containing increasing concentrations of the analytes under optimized conditions. The plots of peak area *versus* analyte concentration yielded linear regression equations, from which the slope, intercept, and correlation coefficient (R^2) were calculated to confirm linearity. The results demonstrated a clear linear relationship between the analyte concentration and detector response within the range of 10.0–900.0 ng mL^{-1} for both drugs. Representative calibration plots for GLZ and GLM are presented in Fig. 9.

The LOD represents the lowest concentration at which the analyte can be confidently detected but not necessarily quantified, while the LOQ denotes the lowest concentration that can be determined with acceptable precision and accuracy. The data indicate that, following enrichment, the signal intensities increased proportionally with concentration, confirming both the efficiency of the preconcentration procedure and the reliability of the HPLC-DAD measurements.

3.4. Application of the developed method in real samples

The developed method was validated using the synthetic and human urine samples as sample media. The urine samples

Table 4 Pictograms related to the herein reported procedure highlighting the applicability and the green profile by means of different internationally accepted tools

Tool	Pictogram	Notes
AGREE		Quite green procedure based on the 12 principles of the Green Analytical Chemistry (GAC). With an AGREE score of **0.66**, the method demonstrates **moderate greenness**, showing acceptable sustainability but requiring further optimization.
ComplexMoGAPI	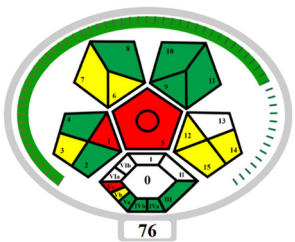	Since the Complex MoGAPI score is **76**, which falls within the **60–80 range**, the method can be evaluated as "**good green**". It exhibits satisfactory environmental performance and aligns well with green analytical principles
BAGI		The score higher than 60 highlights that the method can be considered "practical"
CACI	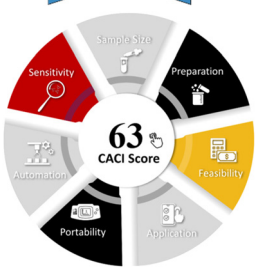	Applications with a CACI score between 50% and 75% are considered acceptable in terms of practicality. The score equal to 63 highlights that the method can be considered "practical" as also highlighted by BAGI

from a healthy volunteer, who abstained from any medication and provided informed consent regarding the experimental procedure and the nature of the study, were collected into capped test tubes and immediately analyzed.

Three different concentration levels of standards (200 and 400 ng mL^{-1}) were spiked into synthetic and human urine samples separately, and recovery experiments were conducted using these samples (Table 3). Recovery values were obtained in the range of 98.1–102.2% while RSD values were lower than 5.3%. The application of the developed method to spiked and real urine samples yielded satisfactory recoveries, with the quantitative results provided in Table 3, demonstrating the suitability of the method for practical biological sample analysis.

The obtained validation parameters confirmed that the proposed MSPE–HPLC-DAD method offers high sensitivity, good reproducibility, and excellent applicability for trace-level quantification of GLZ and GLM in complex biological matrices.

3.5. Greenness and applicability assessment

The developed MSPE–HPLC-DAD method has been evaluated by means of several useful indexes to present its environmentally friendly and practice properties. The environmental sustainability and operational efficiency of the procedure were examined through the AGREE,[55] complex modified GAPI,[56] and practical feasibility and overall environmental performance of the method using the BAGI[57] and CACI[58] indices. The collective outcomes of these evaluations, highlighting the method's minimal solvent requirement, reduced waste generation, and high analytical efficiency, are summarized in Table 4.

4. Conclusion

A new and environmentally sustainable analytical approach was developed for the trace determination of two oral antidiabetic drugs, GLZ and GLM, based on the combination of magnetic solid-phase extraction (MSPE) and high-performance liquid chromatography with diode array detection (HPLC-DAD). The method was designed to achieve efficient preconcentration, selective isolation, and accurate quantification of target molecules in complex biological matrices. The use of magnetic nanoparticles enabled rapid phase separation, minimized solvent consumption, and allowed the overall analytical workflow to be conducted using simple and widely available laboratory equipment.

Magnetic APTES–sulfanilamide was deliberately designed as a suitable sorbent platform by integrating a versatile silanization layer with a structurally compatible recognition functionality. APTES was employed to introduce surface amine groups onto Fe_3O_4 nanoparticles, enabling stable covalent immobilization and providing active interaction sites. Subsequent sulfanilamide functionalization was strategically selected due to its structural resemblance to sulfonylurea antidiabetic drugs. The sulfanilamide moiety contains hydrogen bond donor and acceptor sites, polar sulfonyl groups, and aromatic regions capable of establishing multiple intermolecular interactions with target analytes. These include hydrogen bonding, dipole–dipole interactions, and hydrophobic association, collectively enhancing adsorption affinity and extraction selectivity. Compared with conventional magnetic sorbents lacking molecularly compatible ligands, this dual-functional design offers improved recognition capability toward sulfonylurea compounds.

The proposed method demonstrated excellent linearity across the 10.00–900.00 ng mL^{-1} range, with correlation coefficients (R^2) exceeding 0.9901 for both analytes. The limits of detection (LOD) and quantification (LOQ) were substantially improved after MSPE, decreasing from the microgram to nanogram per milliliter level. Precision studies revealed RSD values below 3.5%, confirming the repeatability of the procedure. The method's applicability was further validated using synthetic and real urine samples, yielding satisfactory recoveries and proving its reliability for biological analysis.

In addition to its analytical performance, the proposed MSPE–HPLC-DAD system was evaluated through various Green Analytical Chemistry (GAC) metrics, confirming its compliance with eco-friendly practices due to minimal solvent usage and low waste generation. Overall, this study presents the first reported application of MSPE coupled with HPLC-DAD for the chromatographic determination of GLZ and GLM, offering a robust, low-cost, and green alternative for routine pharmaceutical and bioanalytical applications.

Author contributions

Songül Ulusoy: writing, original draft, data curation, validation, review and editing. Şule İrem Altunbaş :formal analysis, validation. Aslıhan Gürbüzer: conceptualization, review. Ümmügülsüm Polat: methodology, formal analysis. Halil İbrahim Ulusoy: data curation, supervision, project administration, editing, and funding acquisition.

Conflicts of interest

The authors declare that they have no conflict of interest.

Consent for publication

All authors have read and agreed to the published version of the manuscript.

Data availability

All data generated or analyzed during this study are included in this published article and its supplementary information files.

Acknowledgements

This study was completed with support provided from projects by Sivas Cumhuriyet University Scientific Research Projects Commission as a research project (Codes: ECZ-2021–082). This study was carried out as the thesis project of Şule İrem Altunbaş, a fifth-year student at the Faculty of Pharmacy, as part of her Research Project course. Additionally, the study was also supported by TÜBİTAK 2209-A Student Research Projects under the project number [1919B012112121]. The authors would like to express their sincere gratitude to Dr Gökhan Sarp for his valuable contributions to the characterization studies of the synthesized magnetic material. His expertise and insightful discussions significantly enriched the experimental part of this work and are deeply appreciated. Language editing support was provided by ChatGPT (OpenAI), which was used to improve the linguistic accuracy and fluency of selected English sections of the manuscript. No content was generated or interpreted by the tool.

References

1 H. Zhang, K. Colclough, A. L. Gloyn and T. I. Pollin, *J. Clin. Invest.*, 2021, **131**, e142244.
2 D. Care and S. S. Suppl, *Diabetes Care*, 2022, **45**, 17–38.
3 N. Rakieten, M. L. Rakieten and M. R. Nadkarni, *Cancer Chemother. Rep., Part 1*, 1963, **29**, 91–98.
4 M. H. Tanrıverdi, T. Çelepkolu and H. Aslanhan, *J. Clin. Trials Exp. Invest.*, 2015, **4**, 562–567.
5 F. Hill-Briggs, N. E. Adler, S. A. Berkowitz, M. H. Chin, T. L. Gary-Webb, A. Navas-Acien, P. L. Thornton and D. Haire-Joshu, *Diabetes Care*, 2021, **44**, 258–279.
6 N. El-Enany, *Farmaco*, 2004, **59**, 63–69.
7 F. Magni, L. Marazzini, S. Pereira, L. Monti and M. G. Kienle, *Anal. Biochem.*, 2000, **282**, 136–141.
8 L. M. F. P. Moraes, G. A. Pianetti, I. D. C. César and C. Fernandes, *J. AOAC Int.*, 2017, **100**, 1420–1427.
9 M. AlShehri, N. Al Zoman, H. AlHarbi, K. AlSulaihim and F. AlOdaib, *J. Chem. Soc. Pak.*, 2017, **39**, 541–546.
10 B. R. Nagulancha and K. R. Vandavasi, *Biomed. Chromatogr.*, 2023, **37**, 1–13.
11 S. Altinöz and D. Tekeli, *J. Pharm. Biomed. Anal.*, 2001, **24**, 507–515.
12 L. Michalcová and Z. Glatz, *J. Sep. Sci.*, 2016, **39**, 3631–3637.
13 S. G. Han and T. G. Nam, *Appl. Biol. Chem.*, 2024, **67**, 12.
14 T. Rejczak and T. Tuzimski, *Food Anal. Methods*, 2017, **10**, 3666–3679.
15 H. S. Yang, A. H. B. Wu, K. L. Johnson-Davis and K. L. Lynch, *Clin. Chim. Acta*, 2016, **454**, 130–134.
16 C. H. Xu, G. S. Chen, Z. H. Xiong, Y. X. Fan, X. C. Wang and Y. Liu, *TrAC, Trends Anal. Chem.*, 2016, **80**, 424–435.
17 M. Yu, A. Roszkowska and J. Pawliszyn, *ACS Environ. Au*, 2022, **2**, 30–41.
18 T. Tuzimski and T. Rejczak, *Food Chem.*, 2016, **196**, 1343–1349.
19 D. A. Lambropoulou and T. A. Albanis, *Anal. Bioanal. Chem.*, 2007, **389**, 1663–1683.
20 J. Płotka-Wasylka, N. Szczepańska, M. de la Guardia and J. Namieśnik, *TrAC, Trends Anal. Chem.*, 2015, **73**, 19–38.
21 C. F. Poole, *TrAC, Trends Anal. Chem.,*, 2003, **22**, 362–373.
22 A. L. Capriotti, C. Cavaliere, G. La Barbera, C. M. Montone, S. Piovesana and A. Laganà, *Friedr. Vieweg und Sohn Verlags GmbH*, 2019, preprint, DOI: 10.1007/s10337-019-03721-0.
23 M. Wierucka and M. Biziuk, *TrAC, Trends Anal. Chem.*, 2014, **59**, 50–58.
24 Y. Yamini, E. Tahmasebi and L. Ranjbar, *Biol. Trace Elem. Res.*, 2012, **147**, 378–385.
25 S. D. Abkenar, M. Khoobi, R. Tarasi, M. Hosseini, A. Shafiee and M. R. Ganjali, *J. Environ. Eng.*, 2015, **141**, 1–7.
26 Q. Gao, C. Y. Lin, D. Luo, L. L. Suo, J. L. Chen and Y. Q. Feng, *J. Sep. Sci.*, 2011, **34**, 3083–3091.
27 S. Khan, S. Hussain, A. Wong, M. V. Foguel, L. M. Gonçalves, M. I. P. Gurgo and M. D. P. Sotomayor, *Reactive Funct. Polym.*, 2018, **122**, 175–182.
28 R. Zhang, S. Wang, Y. Yang, Y. Deng, D. Li, P. Su and Y. Yang, *Anal. Bioanal. Chem.*, 2018, **410**(16), 3779–3788.
29 Q. Li, M. H. W. Lam, R. S. S. Wu and B. Jiang, *J. Chromatogr. A*, 2010, 1219–1226.
30 Ö. Demir, H.İ Ulusoy, Ü. Polat and S. Ulusoy, *Curr. Anal. Chem.*, 2023, **19**, 472–481.
31 S. Ulusoy, E. Yilmaz, Z. Erbas, H. I. Ulusoy and M. Soylak, *Sep. Sci. Technol.*, 2019, **55**, 2025–2036.
32 S. Ulusoy, M. Locatelli, A. Tartaglia, A. Kabir and H. İ Ulusoy, *Chem. Pap.*, 2022, **76**, 3649–3659.
33 Ş. Temiz, S. Ulusoy, H. İ. Ulusoy, E. Durgun, Ü. Polat and G. Sarp, *J. Chromatogr. B:Anal. Technol. Biomed. Life Sci.*, 2025, **1251**, 124404.
34 R. R. Naredla and D. A. Klumpp, *Tetrahedron Lett.*, 2013, **54**, 5945–5947.
35 M. F. Cheira, *SN Appl. Sci.*, 2020, **2**, 398.
36 H. I. Ulusoy, U. Polat and S. Ulusoy, *RSC Adv.*, 2023, **13**, 20125–20134.
37 Ö. Demir, H.İ Ulusoy, Ü. Polat and S. Ulusoy, *Curr. Anal. Chem.*, 2023, **6**, 472–481.
38 S. Ulusoy, M. Locatelli, A. Tartaglia, A. Kabir and H. İ Ulusoy, *Chem. Pap.*, 2022, **6**, 3649–3659.
39 S. Cotillas, E. Lacasa, C. Sáez, P. Cañizares and M. A. Rodrigo, *Water Res.*, 2018, **128**, 383–392.
40 L. O. Paula, A. C. Sene, L. A. Manfroi, A. A. Vieira, M. A. R. Ramos, N. K. Fukumasu, P. A. Radi and L. Vieira, *J. Bio- Tribo-Corros.*, 2018, **4**, 51.
41 H. İ. Ulusoy, E. Yılmaz and M. Soylak, *Microchem. J.*, 2019, **145**, 843–851.
42 K. Althumayri, A. Guesmi, W. A. El-Fattah, A. Houas, N. Hamadi and A. Shahat, *ACS Omega*, 2023, **8**, 6762–6777.
43 N. Bijari, M. Falsafi, K. Pouraghajan and R. Khodarahmi, *J. Biomol. Struct. Dyn.*, 2021, **39**, 7093–7106.
44 M. Sypabekova, A. Hagemann, D. Rho and S. Kim, *Biosensors*, 2023, **13**, 36.

45 R. C. Popescu, E. Andronescu and B. S. Vasile, *Nanomaterials*, 2019, **9**, 1–31.
46 F. U. Eze, C. J. Ezeorah, B. C. Ogboo, O. C. Okpareke, L. Rhyman, P. Ramasami, S. N. Okafor, G. Tania, S. Atiga, T. U. Ejiyi, M. C. Ugwu, C. P. Uzoewulu, J. I. Ayogu, O. C. Ekoh and D. I. Ugwu, *Molecules*, 2022, **27**, 1–17.
47 M. A. Bedair, A. M. Abuelela, M. Alshareef, M. Owda and E. M. Eliwa, *RSC Adv.*, 2022, **13**, 186–211.
48 L. Bondarenko, E. Illés, E. Tombácz, G. Dzhardimalieva, N. Golubeva, O. Tushavina, Y. Adachi and K. Kydralieva, *Nanomaterials*, 2021, **11**, 1418.
49 C. Comanescu, *Coatings*, 2023, **13**, 1–31.
50 B. D. C. Mapa, L. U. Araújo, N. M. Silva-Barcellos, T. G. Caldeira and J. Souza, *Appl. Sci.*, 2020, **10**, 7131.
51 B. A. Caine, M. Bronzato and P. L. A. Popelier, *Chem. Sci.*, 2019, **10**, 6368–6381.
52 B. Zhang, Y. Wang, J. Zhang, S. Qiao, Z. Fan, J. Wan and K. Chen, *Colloids Surf., A*, 2020, **586**, 124288.
53 S. Villa, P. Riani, F. Locardi and F. Canepa, *Materials*, 2016, **9**, 826.
54 International Council for Harmonisation of Technical Requirements for Pharmaceuticals for Human Use (ICH), Title of Document, 2005.
55 W. Wojnowski, M. Tobiszewski, F. Pena-Pereira and E. Psillakis, *TrAC, Trends Anal. Chem.*, 2022, **149**, 116553.
56 F. R. Mansour, K. M. Omer and J. Płotka-Wasylka, *Green Anal. Chem.*, 2024, **10**, 100126.
57 N. Manousi, W. Wojnowski, J. Płotka-Wasylka and V. Samanidou, *Green Chem.*, 2023, **25**, 7598–7604.
58 F. R. Mansour, A. Bedair and M. Locatelli, *Adv. Sample Prep.*, 2025, **14**, 100164.